Journal of Molecular Structure 1135 (2017) 197–201

Contents lists available at ScienceDirect

Journal of Molecular Structure

journal homepage: http://www.elsevier.com/locate/molstruc

# Orientation towards asymmetric transfer hydrogenation of ketones catalyzed by (pyrazolyl)ethyl)pyridine Fe(II) and Ni(II) complexes

Makhosazane N. Magubane [a], Mohd Gulfam Alam [a], Stephen O. Ojwach [a, *], Orde Q. Munro [b]

[a] School of Chemistry and Physics, University of KwaZulu-Natal, Pietermaritzburg Campus, Private Bag X01 Scottsville, 3209, South Africa
[b] School of Chemistry, University of the Witwatersrand, PO WITS, 2050, Johannesburg, South Africa

ARTICLE INFO

*Article history:*
Received 7 December 2016
Received in revised form
21 January 2017
Accepted 22 January 2017
Available online 26 January 2017

*Keywords:*
Nickel
Iron
Pyrazolyl
Transfer hydrogenation
Ketones

ABSTRACT

Compounds 2-[1-(3,5-dimethylpyrazol-1-yl)ethyl]pyridine (**L1**) and 2-[1-(3,5-diphenylpyrazol-1-yl) ethyl]pyridine (**L2**) were obtained in a three-step procedure which involved the reduction of acetylpyridine using $NaBH_4$, chlorination of the alcohol intermediate using $SOCl_2$ and subsequent reaction with appropriate pyrazoles. Reactions of **L1** and **L2** with Ni(II) and Fe(II) halides produced the respective complexes Ni(**L1**)$Br_2$ (**1**), Ni(**L1**)$Cl_2$ (**2**), Fe(**L1**)$Cl_2$ (**3**) and Ni(**L2**)$Br_2$ (**4**) as racemic mixtures in moderate yields. The molecular structures of complexes **1** and **4** are dinuclear and mononuclear respectively. All the complexes (**1**–**4**) formed active catalysts for the transfer hydrogenation of ketones (THK) in 2-propanol at 82 °C affording conversions of 58%–84% within 48 h. The influence of catalyst structure, reaction conditions and identity of ketone substrates in the TH reactions have been successfully established.



## 1. Introduction

Asymmetric transfer hydrogenation of ketones (ATHK) is a well-established method used to achieve enantiomerically enriched secondary alcohols [1,2]. Optically active alcohol products are useful intermediates in the manufacture of fine chemicals especially pharmaceuticals and pesticides [3,4]. Noyori and co-workers [1] first reported the Ru(II) complex [RuCl(η6-arene)(N-arylsulfonyl-DPEN)] as a catalyst in the transfer hydrogenation of ketones [5] to afford optically active products with high stereoselectivity. Since this discovery, there has been an extraordinary chiral catalyst development and applications in the asymmetric transfer hydrogenation reactions of ketones [6].

Currently, we have been working on the design and development of ruthenium, nickel and iron metal complexes as catalysts in the transfer hydrogenation of ketones [7]. In this current contribution, we originally aimed to design chiral (pyrazolyl)pyridine ligands and their Ni(II) and F(II) complexes as possible stereoselective catalysts for asymmetric transfer hydrogenation of ketones. However, out attempts to isolate the chiral ligands using Corey-Bakshi-Shibata (CBS) as the reducing agent have been so far unsuccessful. Other reports on the challenges of stereoselective reduction of acetylpyridine [8,9] have also been published. Herein, we thus report the syntheses of racemic mixtures of these pyrazolyl compounds, their respective Ni(II) and Fe(II) complexes and applications as catalysts in the transfer hydrogenation of various ketones.

## 2. Experimental

### 2.1. Materials and methods

The chemicals $NiCl_2$, $NiBr_2$, $FeCl_2 \cdot 4H_2O$, 2-acetylpyridine, $SOCl_2$, $NaBH_4$ were obtained from Sigma-Aldrich and used as received. The solvents; dichloromethane, isopropanol, absolute ethanol and deuterated solvents were bought from Merck Chemicals, distilled and dried using conventional methods. NMR spectra were recorded on a Bruker 400 MHz ($^1H$) and a 100 MHz ($^{13}C$) spectrometer. Elemental analyses were performed on Thermal Scientific Flash 2000 and mass spectra were recorded on LC Premier micro-mass Spectrometer. Magnetic moment measurements were performed in an Evans balance.

### 2.2. Syntheses2-[1-(3,5-dimethylpyrazol-1-yl)ethyl]pyridine (*L1*)

Compound **L1** was prepared by dissolving 2-(1-chloroethyl)

* Corresponding author.
*E-mail address:* ojwach@ukzn.ac.za (S.O. Ojwach).

http://dx.doi.org/10.1016/j.molstruc.2017.01.068
0022-2860/

pyridine, initially prepared by reduction of acetyl pyridine using $NaBH_4$ and subsequent reaction with $SOCl_2$, (2.02 g, 14.20 mmol) and 3,5-dimethylpyrazole (1.37 g, 14.20 mmol) in toluene (30 mL), 40% aqueous NaOH (10 mL) and 40% aqueous tetrabutylammonium bromide (5–6 drops). The reaction mixture was refluxed for 120 h. The organic layer was then separated from the aqueous layer and washed three times with deionised water, then dried over anhydrous $Na_2SO_4$ and solvent removed under vacuum. Purification of the crude product by column chromatography using a solution of hexane and diethyl ether mixture (3:2) gave a chrome yellow liquid. Yield: 1.43 g (49%). $^1$H NMR ($CDC1_3$): δ 2.14 (s, 3H, $CH_3$, pz); 2.30 (s, 3H, $CH_3$, pz); 1.96 (d, 3H, $CH_3$, $^3J_{HH}$ = 8); 5.46 (q, H, $CH_3$); 5.87 (s, 1H, pz); 6.82 (d, $^1$H, py, $^3J_{HH}$ = 7.61 Hz); 7.15 (t, $^1$H, py, $^3J_{HH}$ = 7.8 Hz); 7.58 (t, $^1$H, py, $^3J_{HH}$ = 7.8 Hz); 8.54 (d, $^1$H, py, $^3J_{HH}$ = 7.8 Hz).$^{13}$C NMR (100 MHz, $CDCl_3$) δ: 13.71, 14.05, 20.19, 59.17, 105.64, 120.25, 122.13, 137.07, 139.49, 147.50, 148.77, 162.10. (ESI-MS) *m/z* (%) 201 ($M^+$, 35%).

### 2.3. Synthesis of 2-[1-(3,5-diphenylpyrazol-1-yl)ethyl]pyridine (*L2*)

Compound **L2** was prepared following the same method described for **L1** using 2-(1-chloroethyl)pyridine (2.00 g, 14.30 mmol) and 3,5-diphenylpyrazole (3.14 g, 14.30 mmol). Light red semi-solid. Yield: 1.68 (36%). $^1$H NMR ($CDC1_3$): δ 2.02 (d, 3H, $CH_3$); 5.67 (q, 1H, CH); 6.67 (s, 1H, CH, pz); 7.16 (d, 1H, py, $^3J_{HH}$ = 7.61 Hz); 7.93 (d, 1H, py, $^3J_{HH}$ = 7.8 Hz); 7.61 (t, 2H, py, $^3J_{HH}$ = 7.73 Hz), 7.36–7.45 (m, 10H, Ph). $^{13}$C NMR (100 MHz, $CDCl_3$) δ: 20.04, 59.57, 103.63, 120.93, 122.19, 125.61, 125.63, 125.69, 127.61, 128.40, 128.57, 128.65, 128.69, 128.94, 129.05, 130.50, 133.74, 137.18, 145.69, 148.56, 150.80, 161.95. (ESI-MS) *m/z* (%) 348 ($M^+$+Na, 75%).

### 2.4. Synthesis of complex [$Ni_2$(*L1*)$_2Br_2$(μ-Br)$_2$] (*1*)

To a mixture of $NiBr_2$ (0.11 g; 0.50 mmol) in $CH_2Cl_2$ (10 mL) was added a solution of **L1** (0.10 g; 0.50 mmol) in $CH_2Cl_2$ (10 mL). The mixture was stirred for 24 h at room temperature to give a purple solution. Slow evaporation of the solution afforded purple crystals suitable for single crystal X-ray analyses. Yield = 0.15 g (73%). ESI-MS), *m/z* (%) 339 (1/2 $M^+$ – Br, 15%), 259 (1/2 $M^+$ – $Br_2$, 5%). $\mu_{eff}$ = 2.96 BM. Anal Cald. $C_{24}H_{30}Br_4N6Ni_2$. C, 34.34; H, 3.60; N, 10.01. Found: C, 34.11; H, 3.80; N, 10.32.

Complexes **2**–**4** were prepared following the protocol described for **1**.

### 2.5. Synthesis of complex [$Ni_2$(*L1*)$_2Cl_2$(μ-Cl)$_2$] (*2*)

$NiCl_2$ (0.06 g; 0.50 mmol) and **L1** (0.16 g; 0.50 mmol). Orange solid. Yield = 0.12 g (65%). (ESI-MS), *m/z* (%) 295 (1/2 $M^+$ – Cl, 75%). $\mu_{eff}$ = 2.95 BM. Anal. Cald for $C_{24}H_{30}Cl_4N_6Ni_2$: C, 43.56; H, 4.57; N, 12.70. Found: C, 43.29; H, 4.78; N, 12.97.

### 2.6. Synthesis of complex [$Fe_2$(*L1*)$_2Cl_2$(μ-Cl)$_2$] (*3*)

**3**: $FeCl_2$ (0.10 g; 0.50 mmol) and **L1** (0.10 g; 0.50 mmol). Dark brown solid. Yield = 0.08 g (51%). (ESI-MS), *m/z* (% abundance) 464 (1/2 $M^+$ – Cl, 8%). $\mu_{eff}$ = 5 0.00 BM. Anal. Cald for $C_{24}H_{30}Cl_4Fe_2N_6$: C, 43.94; H, 4.61; N, 12.81. Found: C, 43.49; H, 4.90; N, 13.02.

### 2.7. Synthesis of complex [$Ni_2$(*L2*)$Br_2$] (*4*)

$NiBr_2$ (0.10 g; 0.46 mmol) and **L1** (0.15 g; 0.46 mmol) were used. Purple solid. Yield = 0.17 g (67%). (ESI-MS), *m/z* (% abundance) 464 ($M^+$ – Br, 11%), 384 ($M^+$ – $Br_2$, 5%), 325 ($M^+$ – $NiBr_2$, 10%), 311 ($M^+$ – $NiBr_2$,-$CH_3$, 18%) $\mu_{eff}$ = 3.62 BM. Anal. Cald for $C_{22}H_{19}Br_2N_3Ni$: C, 48.58; H, 3.52; N, 7.73. Found: C, 48.78; H, 3.21; N, 7.48.

### 2.8. Crystal data collection and structure refinement

Single crystal X-ray diffraction data collection and refinement for complex **1** and **4** were recorded on a Bruker Apex Duo equipped with an Oxford Instruments Cryo jet operating at 100 (2) K and an Incoatec micro source operating at 30 W power. The data were collected with Mo Kα (λ = 0.71073 Å) radiation at a crystal-to-detector distance of 50 mm. The following conditions were used for the data collection: omega and phi scans with exposures taken at 30 W X-ray power and 0.50° frame widths using APEX2 [10]. The data were reduced with the programme SAINT [10] using outlier rejection, scan speed scaling, as well as standard Lorentz and polarization correction factors. A SADABS semi-empirical multi-scan absorption correction was applied to the data. Direct methods, SHELXS-2014 [11] and WinGX [12] were used to solve all three structures. All non-hydrogen atoms were located in the difference density map and refined anisotropically with SHELXL-2014 [11]. All hydrogen atoms were included as idealized contributors in the least squares process. Their positions were calculated using a standard riding model with C-$H_{aromatic}$ distances of 0.93 Å and $U_{iso}$ = 1.2 Ueq.

## 3. Results and discussion

### 3.1. Syntheses and spectroscopic characterization of the compounds

The pyrazolyl ligands **L1** and **L2** were prepared following a conventional method for the reduction of ketones using $NaBH_4$ as shown in Scheme 1. Purification of the crude products using column chromatography and hexane:diethyl ether (3:2) solvent system afforded **L1** and **L2** as analytically pure compounds in low yields. $^1$H NMR spectra of both **L1** and **L2** showed a quartet at 5.46 ppm and 5.67 ppm respectively which were assigned to the methine protons. All the expected signals were observed in the $^1$H NMR spectra of both compounds **L1** and **L2** (Fig. S1).

Treatment of compounds **L1** and **L2** with the relevant Ni(II) or Fe(II) salts afforded the corresponding complexes **1**–**4** in moderate

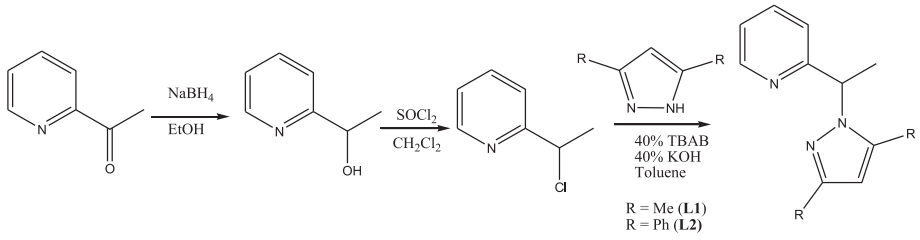


**Scheme 1.** The synthetic route for ligands **L1** and **L2** using $NaBH_4$ as the reducing agent.

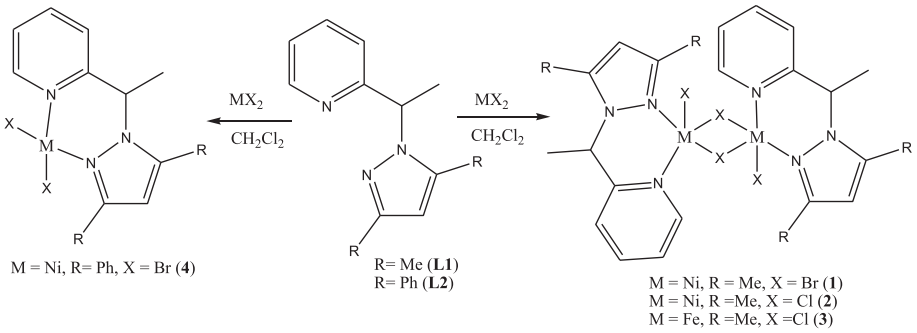


**Scheme 2.** Synthesis of Ni(II) and Fe(II) complexes **1**–**4** of pyrazolyl ligands **L1** and **L2**.

to good yields (Scheme 2). While the Ni(II) complexes **1**–**3** containing less bulky ligand **L1** exhibited dimeric solid state structures, complex **4** bearing the bulky phenyl ligand **L2** was monomeric, consistent with structural dependence on steric factors as previously reported for (pyrazol-1-ylmethyl)pyridine Ni(II) complexes [13]. All the complexes (**1**–**4**) were paramagnetic hence we employed magnetic moment measurements, mass spectroscopy (Fig. S2), micro-analyses and single crystal X-ray analyses were to determine their identity and purity.

### 3.2. Crystal structural description of complexes *1* and *4*

Single crystals suitable for X-ray analyses of complexes **1** and **4** were obtained by slow evaporation of their dichloromethane solutions at room temperature. Molecular structures and selected bond parameters for compounds **1** and **4** are shown in Figs. 1 and 2 respectively, while data collection and structural refinement parameters are given in Table 1. The solid state structure of **1** (Fig. 1) is a centrosymmetric dimer and is a five coordinate Ni(II) compound that contains one ligand unit, one terminal and two bridging bromide ligands. Thus the coordination environment about each Ni(II) atom is a distorted square pyramidal.

On the other hand, complex **4** is mononuclear containing two terminal Br ligands and one bidentate **L2** unit to give a four-coordinate number around the metal atom. Thus the coordination geometry about the Ni atom in complex **4** is a distorted tetrahedral. The difference in nuclearity in compounds **1** and **4** may be largely attributed to greater steric demands of the diphenyl ligand **L2** compared to the dimethyl ligand **L1** [14–16].

The average Ni-$N_{pz}$ and Ni-Br distances of 2.0472 Å and 2.4906(3) Å in **1** are slightly longer than those of compound **4** of 2.006(13) Å and 2.364(5) Å respectively. This could be due to

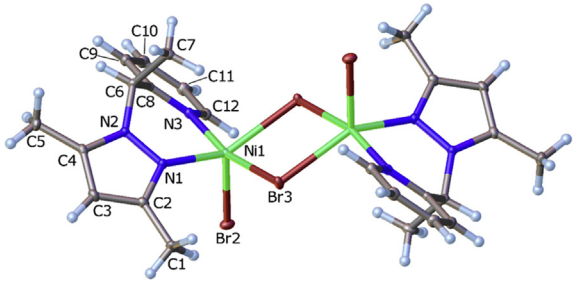


**Fig. 1.** Molecular structure of **1** drawn at 50% probability ellipsoids. Bond lengths (Å): Ni-N(1), 2.0472 (13); Ni-N(3), 2.0587 (13); Ni(1)-Br(2), 2.4329 (3); Ni(1)-Br(3), 2.5483 (3); N(1)-N(2), 1.3709 (17). Bond angles (°):N(1)-Ni(1)-N(3), 89.55 (5); N(1)-Ni(1)-Br(3), 94.32 (4); N(3)-Ni(1)-Br(2), 92.29 (4); N(1)-Ni(1)-Br(2), 100.87 (4); N(3)-Ni(1)-Br(3), 166.15 (4).

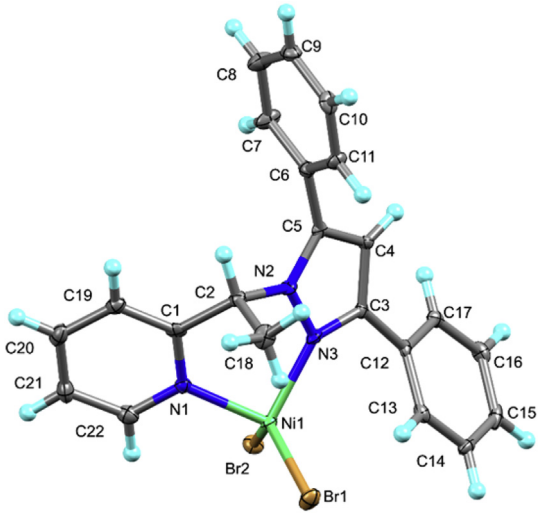


**Fig. 2.** Molecular structure of **4** drawn at 50% probability ellipsoids. Bond lengths (Å): Ni-N(1),2.006(3); Ni-N(3), 1.984(2); Ni(1)-Br(1), 2.3679(5); Ni(1)-Br(2), 2.3601(4); N(2)-N(3), 1.364(3). Bond angles (°): N(1)-Ni(1)-N(3), 92.54(10); N(1)-Ni(1)-Br(2), 104.57(7); N(3)-Ni(1)-Br(2), 108.89(7); N(1)-Ni(1)-Br(1),110.98(7); N(3)-Ni(1)-Br(1), 110.77(7).

**Table 1**
Data collection and structural refinement parameters of complexes **1** and **4**.

| Parameter | **1** | **4** |
|---|---|---|
| Empirical formula | $C_{24}H_{30}Br_4N_6Ni_2$ | $C_{22}$ $H_{19}$ $Br_2$ $N_3$ Ni |
| Formula weight | 839.60 | 543.93 |
| Temperature(K) | 100 | 100 |
| Wavelength (Å) | 0.71073 | 0.71073 |
| Crystal system | Triclinic | Triclinic |
| Space group | *P1* | *Pca*21 |
| *a* (Å) | 8.1757 (5) | 16.5457 (8) |
| *b* (Å) | 8.8004 (6) | 10.4476 (5) |
| *c* (Å) | 11.0344 (7) | 12.0610 (6) |
| α (°) | 82.055 (3) | 90 |
| β (°) | 84.393 (3) | 90 |
| γ (°) | 64.290 (2) | 90 |
| Volume ($A^3$) | 707.82 (8) | 2084.90 (18) |
| Z | 1 | 4 |
| $D_{calcd}$ ($mg/m^3$) | 1.969 | 1.733 |
| Absorption coefficient ($mm^{-1}$) | 7.001 | 4.776 |
| F (000) | 412.0 | 1080 |
| Theta range for data collection (°) | 3.13–28.33 | 1.95 to 26.04 |
| Reflections collected/unique | 25874 | 10162 |
| Completeness to theta | 0.983 | 0.991 |
| Goodness-of-fit on $F^2$ | 1.103 | 0.979 |
| R indices (all data) | $R_1 = 0.0168$ $wR_2 = 0.0436$ | $R_1 = 0.0201$ $wR_2 = 0.0411$ |
| Largest diff. peak and hole (e $Å^{-3}$) | 0.74 and −0.47 | 0.56 and −0.27 |

ligand-ligand repulsions arising from greater shielding/crowding around the Ni atom in **1** compared to **4**. Nonetheless, the bond lengths of Ni-$N_{py}$ of 2.0587(13) Å, Ni-$Br_{(terminal)}$ of 2.4329(3) Å and Ni-$Br_{(bridging)}$ 2.5483 (3) for **1** Å are all statistically similar to the bond lengths reported for similar 2-(pyrazol-1-ylmethyl)pyridine complexes (Figs. 1 and 2). The $N_{pz}$-Ni(1)-$N_{py}$ bond angles about the central atom in **1** of 89.55(5)° is slightly less obtuse than the corresponding $N_{pz}$-Ni(1)-$N_{py}$ bond angle of 92.54(10)° in **4**, consistent with the presence of the more sterically demanding diphenyl ligand **L2** in complex **4**.

### 3.3. Catalytic evaluation of complexes *1*–*4* in transfer hydrogenation of ketones reactions

The Ni(II) and Fe(II) complexes **1**–**4** were investigated as catalysts in the transfer hydrogenation of ketones using KOH as the base and isopropanol as the hydrogen donor (Table 1). All the complexes formed active catalysts in the transfer hydrogenation of acetophenone giving conversions between 58 and 84% in 48 h (Fig. S3). We thus investigated the effects of catalyst structure (Table 2), reaction conditions such as type of base, catalyst concentration (Table 3) and nature of ketone substrate (Table 4) on these transfer hydrogenation reactions.

The nature of the substituent on the pyrazolyl ring and the coordination environment around the metal was noted to have appreciable influence on the catalytic behaviour of the resultant catalysts. While the mononuclear nickel complex **4** gave the highest conversion of 84% corresponding to a TOF of 1750 $h^{-1}$ (Table 2 entry 4), the dinuclear complex **2** was the least active affording conversions of 58%. This trend could be assigned to the steric demands of the two ligand units in the dinuclear complexes **1**–**3** as opposed to one ligand motif in complex **4** [17].

Comparison of complexes **1**–**3** reveals that the Fe complex **3** was the most active displaying conversions of 67% (1404 $h^{-1}$). We attributed this trend to the high reactivity of Fe(II) complexes compared to the Ni(II) analogues [18], usually associated with high electropositivity of Fe(II) [19]. The nature of the halides also controlled the catalytic performance of complexes **1**–**3**; with the bromide complex **1** recording higher catalytic activity than the corresponding dichloride complex **2** (Table 2, entries 1 *vs* 2).

In order to optimise the catalytic reaction conditions of **1**–**4** in the transfer hydrogenation of acetophenone, we studied the influence of catalyst concentration, nature of base using complex **4** (Table 3). We observed that an increase in catalyst concentration from 0.5 mol % to 1.0 mol % resulted in improved catalytic activities from 42% (875 $h^{-1}$) to 84% (1750 $h^{-1}$) (Table 3, entries 1 *vs* 5). However, a further increase in catalyst loading to 1.5 mol % resulted in a slight drop in catalytic activity from 1750 $h^{-}$ to 1688 $h^{-1}$ (Table 3, entries 1 vs 6), usually associated with complex aggregation, thus limiting the number of active species [20]. The impact of the nature of the base was probed by examining the catalytic activities of complex **4** in $^{t}$BuOK, KOH, NaOH and $Na_2CO_3$ (Table 2, entries 1–4). The most active conditions were realized using $^{t}$BuOK, while the least activity was noted using $Na_2CO_3$. This trend is consistent with the order of stability and strengths of the bases and agrees with literature findings where stronger bases give more

**Table 2**
Catalysis data for transfer hydrogenation of ketones by **1**–**4**.[a]

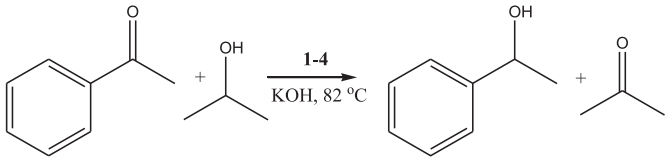


| Entry | Catalyst | Conversion [%][b] | TOF x $10^{-3}$ ($h^{-1}$)[c] |
|---|---|---|---|
| 1 | **1** | 63 | 1319 |
| 2 | **2** | 58 | 1198 |
| 3 | **3** | 67 | 1404 |
| 4 | **4** | 84 | 1750 |

[a] Conditions: acetophenone, 2.0 mmol; catalyst; 0.02 mmol (1.0 mol%); base, 0.4 M KOH in 2-propanol (5 ml); time, 48 h, temperature, 82 °C.[b]Determined by $^{1}$H NMR spectroscopy. [c]Turn over frequency (TOF) = (mmol of substrate)/(mmol of catalyst)/(h).

**Table 3**
Dependence of THK on the type of base and catalyst concentration using complex **4**.[a]

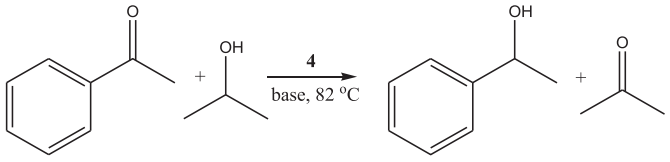


| Entry | Base | Conversion (%)[b] | TOF ($h^{-1}$)[e] |
|---|---|---|---|
| 1 | KOH | 84 | 1750 |
| 2 | NaOH | 80 | 1667 |
| 3 | $Na_2CO_3$ | 24 | 500 |
| 4 | $^{t}$BuOK | 98 | 2042 |
| 5 | KOH | 42[c] | 875 |
| 6 | KOH | 81[d] | 1688 |

[a] Conditions: ketone, 2.00 mmol; catalyst. 0.02 mmol (1 mol%); 0.40 M of base in 2-propanol (5 mL); time, 48 h; temperature, 82 C. [b]Determined by $^{1}$H NMR spectroscopy. [c]0.01 mmol catalyst (0.50 mol%); [d]0.03 mmol catalyst (1.50 mol%). [e]Turn over frequency (TOF) = (mmol of substrate)/(mmol of catalyst)/(h).

**Table 4**
Transfer hydrogenation reactions of different ketone substrate using catalyst **4**.[a]

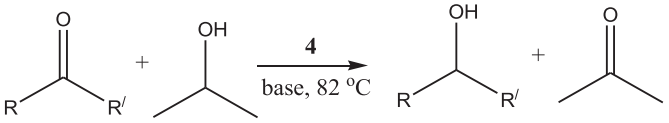


| Entry | Substrate | %Conversion[b] | TOF ($h^{-1}$) |
|---|---|---|---|
| 1 |  | 84 | 1750 |
| 2 |  | 78 | 1625 |
| 3 |  | 88 | 1833 |
| 4 |  | 51 | 1063 |
| 5 | 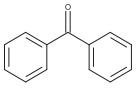 | 72 | 1500 |
| 6 | 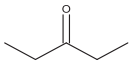 | 35 | 729 |

[a] Conditions: ketone, 2 mmol; catalyst. 0.02 mmol (1 mol%); base, KOH; 0.4 M of KOH in 2-propanol (5 mL), temperature 82 C. [b]Determined by $^{1}$H NMR spectroscopy. TOF = (mmol of substrate)/(mmol of catalyst)/(h).

active catalytic species [21].

The scope of the ketone substrates that can be converted to the respective secondary alcohols was also studied for 2-methylacetophenone, 2-chloroacetophenone, 3-pentanone, benzophenone and 2-methycyclohexanone using complex **4** (Table 4 and Fig. S4). It was noted that changing the ketone substrate resulted in a significant difference in catalytic activity. For instance, conversions of 78% (1625 $h^{-1}$) and 88% (1833 $h^{-1}$) were obtained for 2-methylacetophenone and 2-chloroacetophenone compared to 84% (1750 $h^{-1}$) recorded for acetophenone respectively (Table 4, entries 1–3) and can be assigned to decreased electron density on the C═O bond. These findings are in good agreement with those of Yu et al. [22] in which electron-donating groups give inferior catalytic activities. Significantly, diminished catalytic activities of 51% (1063 $h^{-1}$) and 35% (729 $h^{-1}$) were observed for 2-methycyclohexanone and the aliphatic pentan-3-one respectively. Thus it can be deduced that the aromatic ring plays a role in increasing substrate reactivity [23]. On the other hand, the relatively lower reactivity of 72% (1500 $h^{-1}$) observed for benzophenone compared to acetophenone 84% (1750 $h^{-}$) could attributed to increased ring strain occasioned by the two bulky phenyl rings in benzophenone substrate.

## 4. Conclusions

In summary, we have demonstrated that the reactions of racemic mixtures of 2-[1-(3,5-dimethylpyrazol-1-yl)ethyl]pyridine ligand (**L1**) and 2-[1-(3,5-diphenylpyrazol-1-yl)ethyl]pyridine ligands (**L2**)with $NiCl_2$ or $NiBr_2$ salts produce dinuclear and mononuclear complexes respectively. The catalytic behaviour of complexes **1**–**4** in the transfer hydrogenation of ketones were largely controlled by the coordination environment around the metal atoms in the respective complexes. The optimum conditions and reactivities of various ketones substrates have been successfully established. We believe that this work provides a promising platform for the design of chiral pyrazolyl catalysts for the asymmetric transfer hydrogenation of ketones.

## Acknowledgements

The authors would like to the University of KwaZulu-Natal, and National Research Foundation (NRF), South Africa for financial support.

## Appendix A. Supplementary data

Supplementary data related to this article can be found at http://dx.doi.org/10.1016/j.molstruc.2017.01.068.

## References

[1] R. Noyori, Asymmetric Catalysis in Organic Synthesis, Wiley, New York, 1994, pp. 56–82.
[2] N. Arai, T. Ohkuma, Reduction of carbonyl groups: hydrogenation, in: G.A. Molander (Ed.), Science of Synthesis: Stereoselective Synthesis, second ed., Thieme Stuttgart, Germany, 2010, pp. 9–57.
[3] M. Bullock, An iron catalyst for ketone hydrogenations under mild conditions, Angew. Chem. Int. Ed. 46 (2007) 7360–7363.
[4] J. Vaclavik, P. Sot, B. Vilhanova, J. Pechacek, M. Kuzma, P. Kacer, Practical aspects and mechanism of asymmetric hydrogenation with chiral half-sandwich complexes, Molecules 18 (2013) 6804–6828.
[5] S. Hashiguchi, A. Fujii, J. Takehara, T. Ikariya, R. Noyori, Asymmetric transfer hydrogenation of aromatic ketones catalyzed by chiral ruthenium(II) complexes, J. Am. Chem. Soc. 117 (1995) 7562–7563.
[6] For selected reviews see:. (a) S.E. Clapham, A. Hadzovic, R.H. Morris, Mechanisms of the H2-hydrogenation and transfer hydrogenation of polar bonds catalyzed by ruthenium hydride complexes, Coord. Chem. Rev. 248 (2004) 2201–2237;
(b) R. Malacea, R. Poli, E. Manoury, Asymmetric hydrosilylation, transfer hydrogenation and hydrogenation of ketones catalyzed by iridium complexes, Coord. Chem. Rev. 254 (2010) 729–752;
(c) S. Gladiali, E. Albrico, Asymmetric transfer hydrogenation: chiral ligands and applications, Chem. Soc. Rev. 35 (2006) 226–236.
[7] (a) A.O. Ogweno, S.O. Ojwach, M.P. Akerman, (Pyridyl)benzoazole palladium(II) complexes as homogeneous catalysts in hydrogenation of alkenes and alkynes, Dalton Trans. 43 (2013) 1128–1237;
(b) M.N. Magubane, G.S. Nyamato, S.O. Ojwach, O.Q. Munro, Structural, kinetic, and DFT studies of the transfer hydrogenation of ketones mediated by (pyrazole) pyridine iron (II) and nickel (II) complexes, RSC. Adv. 6 (2016) 65205–65221.
[8] J.G. Quallich, T.M. Woodall, Enantioselective oxazaborolidine reduction of ketones containing heteroatoms, Tetrahedron Lett. 34 (1993) 785–788.
[9] V. Stempaneko, M. Jesus, W. Correa, I. Guzman, C. Vazquez, L. Ortiz, M. Ortiz-Marcials, Highly enantioselective reduction of acetilpyridines and other heteroaromatic ketones with borane and spiroborate esters, Tetrahedron Asymm 18 (2007) 2738–2745.
[10] Bruker. APEX2, SAINT and SADABS, Bruker AXS Inc., Madison, Wisconsin, USA, 2012.
[11] G.M. Sheldrick, Crystal structure refinement with SHELXL, Acta Cryst. A64 (2008) 112.
[12] L.J. Farrugia, WinGX and ORTEP for windows: an update, J. Appl. Cryst. 45 (2012) 849–854.
[13] S.O. Ojwach, I.A. Guzei, L.L. Benade, S.F. Mapolie, J. Darkwa, (Pyrazol-1-ylmethyl) pyridine nickel complexes: ethylene oligomerization and unusual Friedel–Crafts alkylation catalysts, Organometallics 28 (2009) 2127–2133.
[14] W.H. Sun, K. Wang, K. Wedeking, D. Zhang, S. Zhang, J. Cai, Y. Li, Synthesis, characterization, and ethylene oligomerization of nickel complexes bearing N-((Pyridin-2-yl)methylene)quinolin-8-amine derivatives, Organometallics 26 (2007) 4781–4790.
[15] E.C. Alyea, D.W. Meek, Four- and five-coordinate nickel(II) complexes with monodentate phoshines, J. Am. Chem. Soc. 91 (1969) 5761–5768.
[16] A. Terzis, K.N. Raymond, T.G. Spiro, On the structure of $Ni(CN)_5$: raman and infrared evidence, Inorg. Chem. 9 (1970) 2415–2420.
[17] A.R. Karam, E.L. Catari, F.L. Linares, G. Agrifoglio, C.L. Albano, A.D. Barrios, T.E. Lehmann, S.V. Pekerar, L.A. Albornoz, R. Atencio, T. Gonzalez, H.B. Ortega, P. Joskowics, Synthesis, characterization and olefin polymerization studies of iron(II) and cobalt(II) catalysts bearing 2,6-bis(pyrazol-1-yl)pyridines and 2,6-bis(pyrazol-1-ylmethyl) pyridines ligand, Appl. Catal. A Gen. 280 (2005) 165–173.
[18] J.D. Hoeschele, J.E. Turner, W.E. England, Inorganic concepts relevant to metal bonding, activity, and toxicity in a biological system, Sci. Total Environ. 109/110 (1991) 477–492.
[19] K.S. Lee, H.J. Koo, D. Dai, J. Ren, M.H. Whangbo, Electron counting scheme relevant for late transition metal compounds with weakly electronegative ligands. Electronic band structure study of phosphosilicides PtSi3P2 and NiSi2P3, Inorg. Chem. 38 (1999) 340–345.
[20] S.A. Svejda, M. Brookhart, Ethylene oligomerization and propylene dimerization using cationic (alpha-diimine)nickel(II) catalysts, Organometallics 18 (1999) 65–74.
[21] R.N. Prabhu, R. Ramesh, Synthesis, structural characterization, electrochemistry and catalytic transfer hydrogenation of ruthenium(II) carbonyl complexes containing tridentate benzoylhydrazone ligands, J. Organomet. Chem. 718 (2012) 43–51.
[22] S.L. Yu, Y.Y. Li, Z.R. Dong, J.X. Gao, Synthesis of novel chiral tetraaza ligands and their application in enantioselective transfer hydrogenation of ketones, Chin. Chem. Lett. 23 (2012) 395–398.
[23] B. Ak, M. Aydemir, F. Durap, N. Meriç, A. Baysal, The first application of C2-symmetric ferrocenyl phosphinite ligands for rhodium-catalyzed asymmetric transfer hydrogenation of various ketones, Inorg. Chim. Acta 438 (2015) 42–51.